Photoactivation of a nanoporous crystal for on-demand guest trapping and conversion

Hiroshi Sato[1], Ryotaro Matsuda[1,2]★, Kunihisa Sugimoto[3], Masaki Takata[3,4,5] and Susumu Kitagawa[1,2,5,6]★

Porous compounds are ubiquitous and indispensable in daily life as adsorbents and catalysts. The discovery of a new porous compound with unique properties based on intrinsic nanosized space and surface functionalities is scientifically and technologically important. However, the functional species used in this context are limited to those that are sufficiently inert to not spoil the porous structures. Here, we show a new strategy to achieve a crystalline porous material with the pore surface regularly decorated with highly reactive 'bare' nitrenes that are photonically generated from stable 'dormant' precursors at will. The bare triplet nitrenes were accessible to and reacted with adsorbed oxygen or carbon monoxide molecules, which showed not only activation of the pore surface, but also a high probability of chemical trapping and conversion of guest molecules by light stimulation on demand.

Nanoporous compounds have been widely used because of their practical functions for gas storage, separation and molecular catalysis[1]. In particular, sensing or removing toxic, harmful or oxidizing gases (such as CO, NO_x, O_2 and so on) using nanoporous compounds is currently of great importance because of industrial and environmental demands. Surface activity on the nanopore is essential for the porous properties[2,3]. Therefore, a number of attempts have been made to introduce specific functional groups (acid–base sites[4,5], ion-exchange sites[6,7], chemical interaction sites[8–10], hydrogen-bonding sites[11], chiral sites[12–15] and so on) onto the internal surface for fine tuning of the pore environment and metrics. However, the functional species used in this context are limited to those that are sufficiently inert to not spoil the porous structures. This has prevented access to highly reactive functionalities such as electronically open-shell atoms[16], which play a pivotal role in many important chemical transformations but often elude isolation and characterization. Furthermore, if it is possible to activate a nanopore surface by external stimuli where and when desired, on-demand gas storage/trapping systems can be realized.

The keys to success in achieving on-demand activation of porous compounds with a highly reactive pore surface are the following. (1) A stable host framework composed of dormant precursors must be prepared. The dormant precursors should act not only as precursors of reactive species but also as building blocks of porous frameworks. (2) The dormant precursors can be transformed to highly reactive species by external stimuli even in the host framework. (3) The resulting reactive species must be exposed on the pore surface to react or interact with guest molecules, but must be regularly arranged to avoid undesirable reactions with the other parts of the host framework. Therefore, highly designable host porous frameworks are a prerequisite.

From this point of view, we adopted porous coordination polymers (PCPs) or metal–organic frameworks[17–22] as a new platform to create a pore surface with highly reactive species, because of their designability based on various functional metal[23–28] and/or organic[29–34] sites. Reactive open-shell atoms, such as nitrenes, carbenes and radicals, are often seen in intermediate states of useful chemical reactions and could be good candidates for reactive pores. However, control of their stability is a big issue for on-demand systems. Our idea to overcome this problem is to use the photochemical generation method, namely, photoactivation of the pore surface. Aryl azide molecules are among the best candidates as dormant precursor ligands because they can produce highly reactive aryl nitrene[35] without interfering with the other parts in the molecules. In this context, we focused on the design and construction of a PCP framework (CID-N_3; CID: coordination polymers with interdigitated structures) with a photoresponsive aryl azide molecule to achieve a nanoporous compound with a photonically switchable pore surface (Fig. 1a).
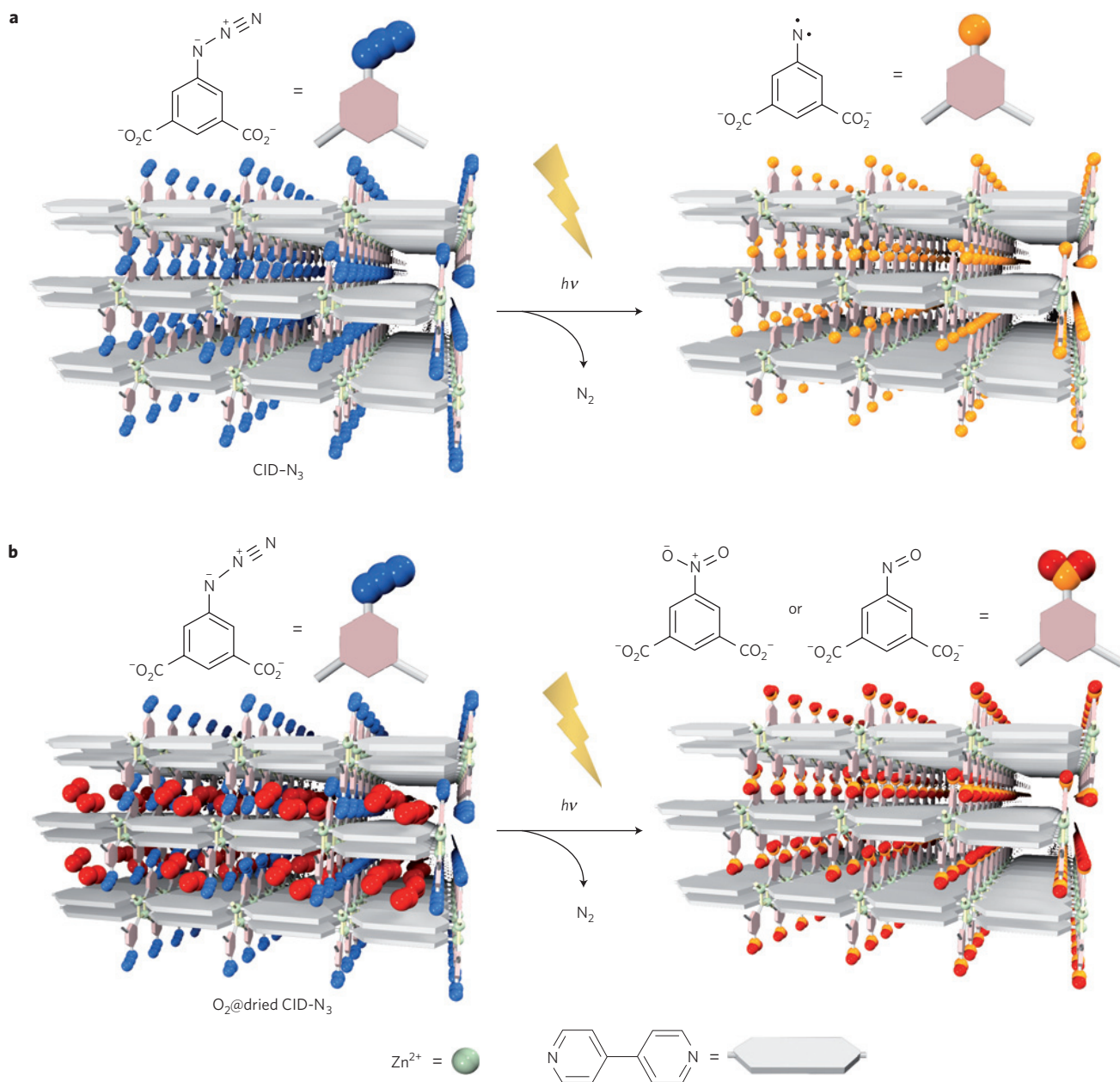
We prepared a linker-type building block with an azide module, 5-azidoisophthalic acid (H_2N_3-ipa), from 5-aminoisophthalic acid by diazotization followed by azidation with sodium azide in a high yield. On the basis of thermogravimetric analysis, H_2N_3-ipa is thermally stable up to $150\,^\circ C$ in the solid form (Supplementary Fig. S1). It is known that irradiation of aryl azides with ultraviolet light ($\lambda \sim 300\,nm$) initially yields singlet aryl nitrenes, which preferentially undergo intersystem crossing to the triplet ground state at low temperature (below 165 K; ref. 35). First, the photochemical reaction of the H_2N_3-ipa ligand in vacuum at 77 K was monitored by *in situ* infrared and electron spin resonance (ESR) measurements. The characteristic stretching bands of the azide group at around $2,110\,cm^{-1}$ in the infrared spectrum (Supplementary Fig. S2a) decreased with ultraviolet irradiation, and ESR-active species that were assignable to a triplet nitrene appeared around 700 mT at 77 K (Supplementary Fig. S3a; ref. 36). Another signal of a biradical, which is a counter-form of the triplet nitrene in equilibrium, was observed in field

661

Figure 1 | Schematic illustration of photoactivation of a PCP with azide functionalities. a,b, The framework of CID-N_3 is formed by interdigitations of two-dimensional sheets composed of Zn^{2+}, 5-azidoisophthalate and 4,4′-bipyridine. Photoactivation of the azide moieties leads to the formation of triplet nitrenes on the pore surface (**a**) and photochemical trapping of physisorbed oxygen molecules in the framework of dried CID-N_3(O_2@dried CID-N_3) (**b**).

around 330 mT (Supplementary Fig. S3a). We synthesized single crystals of a new PCP composed of N_3-ipa ligands as follows: Slow diffusion of a methanol solution of H_2N_3-ipa and 4,4′-bipyridine (bpy) into a *N*,*N*-dimethylformamide (DMF) solution of $Zn(NO_3)_2 \cdot 6H_2O$ afforded block-shaped pale-yellow crystals of $[Zn_2(N_3$-ipa$)_2$(bpy$)_2$(DMF$)_{1.5}]_n$ (CID-N_3) in a few days. As shown in Fig. 2a,b and Supplementary Fig. S4a, the Zn^{2+} ions are in a distorted octahedral geometry, being coordinated by two nitrogen atoms of bpy at the axial positions, two oxygen atoms from the chelating carboxylate of the N_3-ipa and two oxygen atoms from the other N_3-ipa in the equatorial plane. Zn^{2+} and N_3-ipa form one-dimensional double chain structures along the *a* axis and further linkage of these chains through bpy in the axial positions affords two types of infinite two-dimensional sheet (sheet X and sheet Y) (Fig. 2c,d and Supplementary Fig. S4b). In sheet X, the N_3-ipa ligands are located on both sides of the

one-dimensional double chain in a *trans* arrangement (Fig. 2c). In contrast, the N_3-ipa ligands in sheet Y show a *cis* arrangement (Fig. 2d). These two types of two-dimensional sheet are alternately interdigitated to form a stable three-dimensional architecture (Fig. 2e and Supplementary Fig. S4c) through $\pi-\pi$ interactions (distance 3.4 Å) between the planes of the nearest-neighbour N_3-ipa ligands (Fig. 2f,g). A winding one-dimensional channel with a cross-section of 5×6 Å^2 runs along the *c* axis, with aryl azides exposed on the channel surface (Fig. 2e).

We studied the sorption properties of dried CID-N_3, which was obtained by heating the single crystals of CID-N_3 at 120 °C in vacuum for 6 h. The dried CID-N_3 was found to be non-porous for N_2, O_2 and CO at 77 K (Supplementary Fig. S5) because of the slow diffusion of gaseous molecules into the micropore. In contrast, at higher temperature, the adsorption isotherms of N_2, O_2 and CO (at 120 K) and CO_2 and C_2H_2 (at 195 K) showed a steep
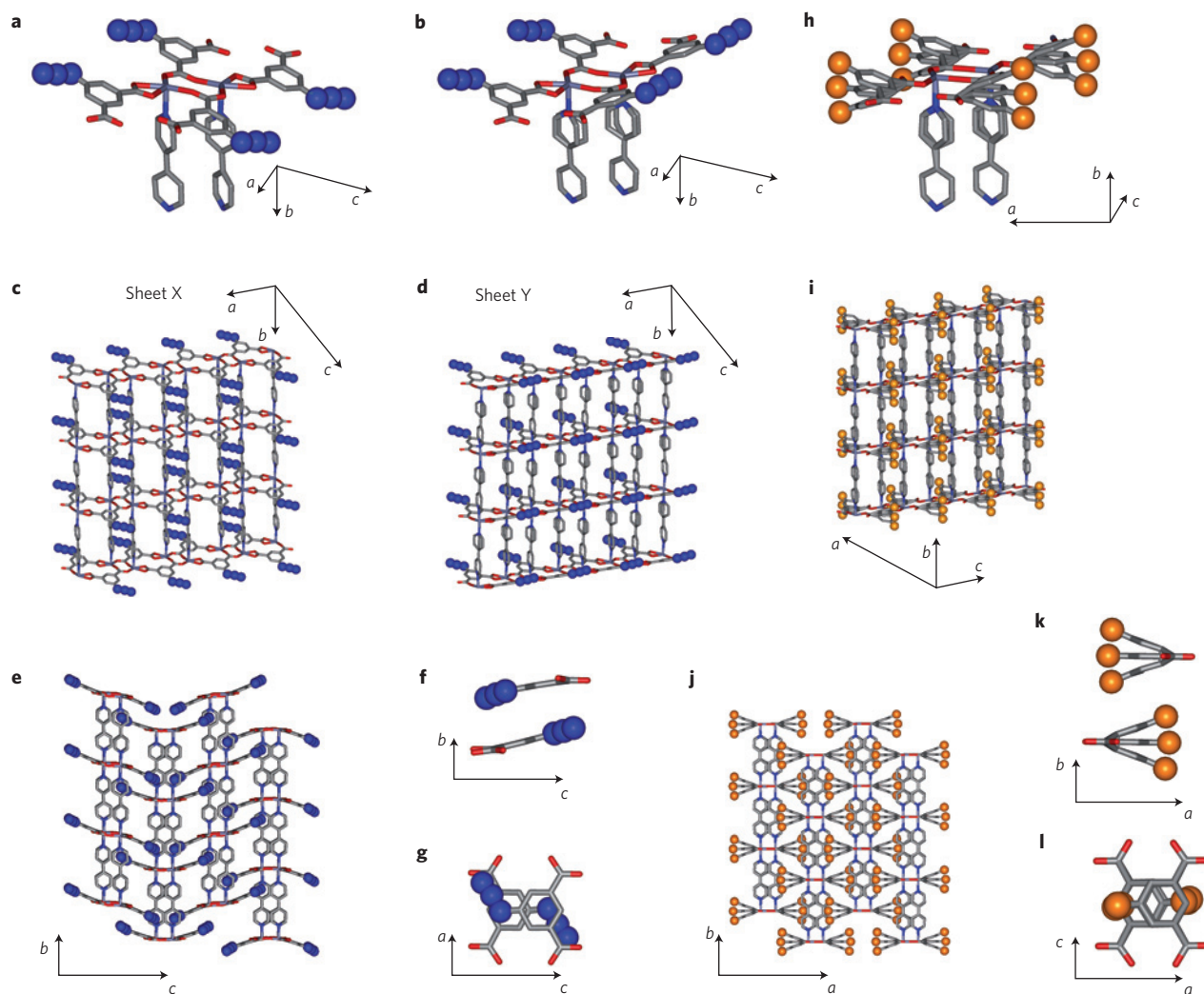
Figure 2 | X-ray crystal structural analyses. a–l, Crystal structures of CID-N_3 (**a–g**) and photoactivated CID-N_3 (**h–l**). Atoms except N atoms of nitrene are coloured as follows: Zn, purple; C, grey; N, blue; O, red. N atoms of the azide are shown as blue balls. N atoms of nitrenes are shown as orange balls. **a,b**, Coordination environment around Zn ions. **c,d**, Views of the two-dimensional sheets (sheets X and Y). **e**, Alternately interdigitated structures viewed along the *a* axis. **f,g**, Neighbouring azide moieties viewed along the *a* and *b* axes, respectively. The guest molecules of DMF and hydrogen atoms are omitted for clarity. **h**, The coordination environment around the Zn ions. **i**, A view of the two-dimensional sheet. **j**, Alternately interdigitated structures viewed along the *c* axis. **k,l**, Neighbouring nitrene moieties viewed along the *c* and *b* axes, respectively. Hydrogen atoms are omitted for clarity. Nitrogen atoms from non-converted azide moieties are also omitted for clarity (**h–l**).

rise in the low relative pressure region and could be categorized as Type I in the International Union of Pure and Applied Chemistry (IUPAC) classification, indicative of typical physisorption by a microporous compound (Supplementary Fig. S6). The adsorbed amounts of N_2, O_2, CO, CO_2 and C_2H_2 were estimated to be 51, 85, 32, 64 and 53 ml(stp) g^{-1} (0.97, 1.60, 0.61, 1.20 and 1.01 molecules per N_3-ipa) at 80 kPa, respectively. These results indicate that the one-dimensional channel has a permanent porosity to accommodate various guest molecules.

We carried out photoirradiation of CID-N_3 and dried CID-N_3 and tried to observe triplet nitrene species in the frameworks by *in situ* measurements of infrared, ESR and single-crystal X-ray diffraction. In the infrared spectra, CID-N_3 and dried CID-N_3 have characteristic stretching bands of the azide group at around 2,110 cm^{-1}, similar to the H_2N_3-ipa ligand. These stretching bands smoothly decreased in intensity to about 35% and 40%, respectively, in 4.5 h with photoirradiation of powdered crystals of CID-N_3 (Fig. 3a) and dried CID-N_3 (Supplementary Fig. S2b) in vacuum at 77 K. Further irradiation did not lead to effective conversion of the azide moieties and 30% of azide moieties still

remained one day after irradiation, which might be attributed to the filtering effect of the generated nitrene species. On the other hand, less change in the C–O stretching band of zinc carboxylate (1,400 cm^{-1}) was observed during photoirradiation, which indicated that these CID structures maintained the basic frameworks composed of carboxylate anions and zinc ions even after photoirradiation. In addition, the ESR measurement also clearly showed the formation of triplet nitrene in CID-N_3 and dried CID-N_3 by photoirradiation (Supplementary Fig. S3b and c). The characteristic signals of triplet nitrene and biradical were observed at field around 700 and 330 mT, respectively, in the ESR spectra of CID-N_3 and dried CID-N_3 after irradiation for 30 min at 77 K. Further clear evidence of the photochemical generation of nitrene species was obtained from crystallographic experiments with synchrotron X-rays at the BL02B1 beamline of SPring-8. We photoirradiated a single crystal of CID-N_3 for 40 min in vacuum at 77 K and observed a clear change in its diffraction image, which was attributed to a crystal transformation in space group in a part of the single crystal from $P2/n$ to $C2/m$ (Supplementary Table S1). The conversion of azide moieties was estimated as 31% in the
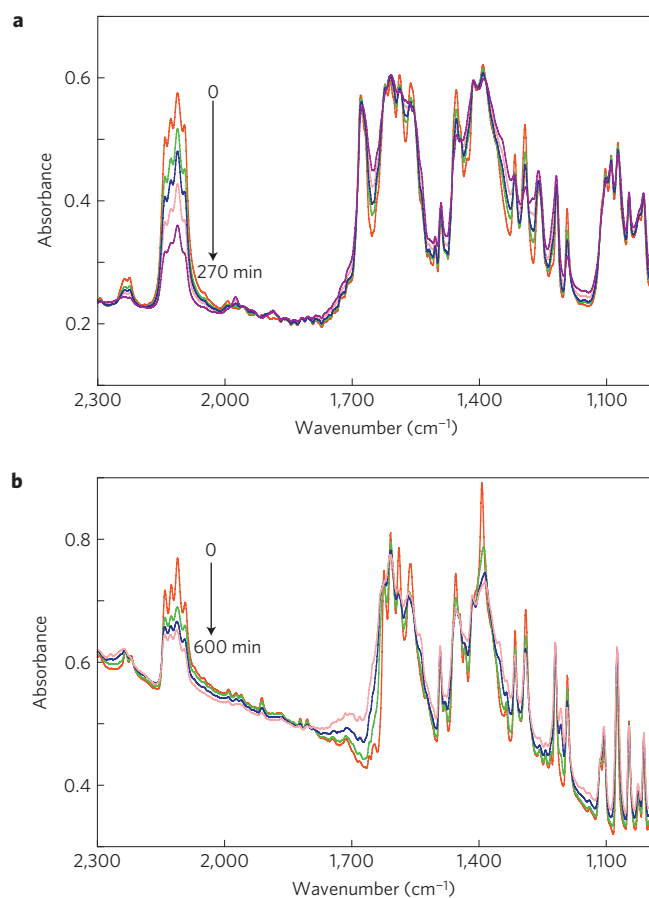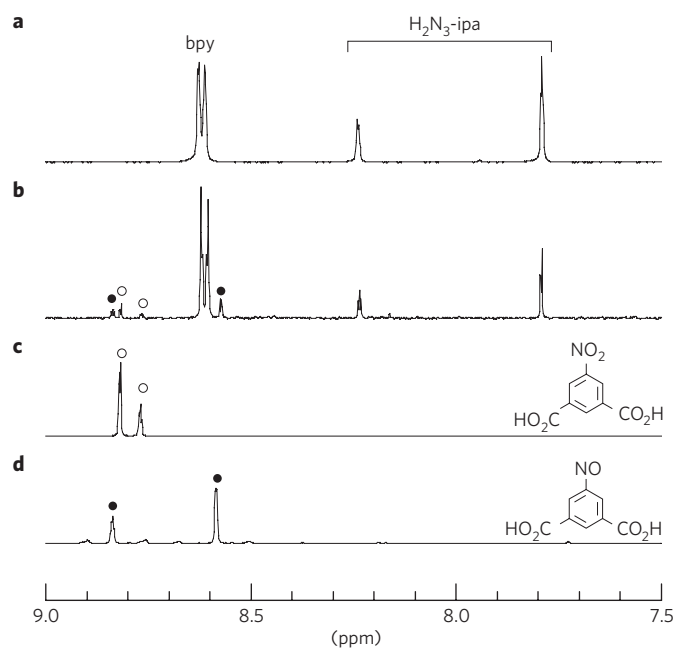
Figure 3 | Photochemical reactions of CID-N$_3$ monitored by infrared measurements. a,b, Photochemical reaction of CID-N$_3$ in vacuum at 77 K (**a**; each spectrum was measured after irradiation for 0, 5, 15, 60 and 270 min) and dried CID-N$_3$ in an O$_2$ atmosphere (80 kPa) at 120 K (**b**; each spectrum was measured after irradiation for 0, 3, 90 and 600 min).

Figure 4 | ^{1}H-NMR study of the photochemical products from dried CID-N$_3$. a,b, ^{1}H-NMR spectra of dried CID-N$_3$ before (**a**) and after (**b**) photoirradiation in an O$_2$ atmosphere (80 kPa) at 120 K for 600 min. **c,d**, ^{1}H-NMR spectra of 5-nitroisophthalic acid (**c**; open circles) and 5-nitrosoisophthalic acid (**d**; filled circles). All of the samples were digested in DMSO-d_6/aq. HCl at 293 K.

transformed structure from structural analysis, and the nitrene generated from N$_3$-ipa ligands showed disorder in three positions (Fig. 2h–l). This could be attributed to decreasing $\pi-\pi$ interactions between aryl planes and neighbouring azide moieties and increasing spaces because of release of the dinitrogen molecule from N$_3$-ipa (Fig. 2k,l). The above-mentioned direct observation indicated that the triplet nitrene anchored on the pore surface was well isolated and sufficiently stable kinetically.

On the basis of the photochemical generation of the highly reactive nitrenes on the pore surface, we sought to demonstrate the usefulness of our porous crystalline material for on-demand photoactivation of the pore surface. We found that the chemical transformation of the adsorbed guest molecules by photoirradiation and photoinduced adsorption of guest molecules are possible.

We carried out photoirradiation on dried CID-N$_3$ in an O$_2$ atmosphere (80 kPa) at 120 K for 10 h and monitored the reactions by infrared spectroscopy. From the infrared spectra, the photochemical conversions of the azide moieties were estimated as 50% for dried CID-N$_3$ (Fig. 3b). We confirmed that the photochemical products from dried CID-N$_3$ were nitro- (NO$_2$-ipa: δ 8.82 and 8.77 ppm) and nitroso- (NO-ipa: δ 8.84 and 8.59 ppm) isophthalic acids by comparing the ^{1}H-NMR spectra of authentic samples with those of the irradiated sample (Fig. 4). It is worth noting that triplet nitrene is well known to react with oxygen to give a nitro compound[37], but few reports about the formation of a nitroso compound by the reaction of nitrene and oxygen have been published[38]. The integral ratio between the signals of

isophthalic acids and bpy indicated that all of the generated nitrene species had reacted with oxygen and converted to either NO$_2$-ipa or NO-ipa. In contrast, the photoirradiation of the ligand molecule (H$_2$N$_3$-ipa) in an O$_2$ atmosphere (Supplementary Fig. S2c) gave a complex mixture found in the ^{1}H-NMR spectrum (Supplementary Fig. S7). These results clearly showed that the porous structure is essential so that the photonically generated nitrene specifically reacts with oxygen to give NO$_2$-ipa and NO-ipa in the solid state (Fig. 1b). Although nitroso groups are known to be converted to other functionalities and can be potentially used for further modification of the pore surface, it is difficult to obtain porous materials that have NO-ipa as a building block using conventional methods because NO-ipa is not stable and gradually converts to a dimerized product, an azoxy compound, in solution. In addition, we have proven that guest trapping by the photogenerated nitrene can be applicable for not only O$_2$ but also other guest molecules, such as CO. In fact, the adsorbed CO molecule reacted with photogenerated nitrene and was converted to isocyanate, which was spectroscopically confirmed[39] (Supplementary Fig. S8).

We demonstrated that *in situ* photoirradiation on dried CID-N$_3$ remarkably impacted on its sorption property. As previously mentioned, the original dried CID-N$_3$ shows almost non-porous behaviour for O$_2$ at 77 K (Fig. 5, isotherm a). However, on *in situ* photoirradiation, the adsorbed amount of O$_2$ significantly increases in the low-pressure region (Fig. 5, isotherm b). An adsorption isotherm of O$_2$ for the completely converted dried CID-N$_3$ is obtained considering the photochemical conversion (15%) estimated from the ^{1}H-NMR spectrum of the photoirradiated sample. According to the isotherms, the photochemically activated dried CID-N$_3$ is able to adsorb 29 times as much O$_2$ at 0.2 kPa compared with the original dried CID-N$_3$, indicating that photoirradiation achieves significant enhancement of the adsorption ability of CID-N$_3$ (Fig. 5, isotherm c).

Our photoactivation method can be used in a wide range of photoreactive species incorporated in PCPs and can be a general
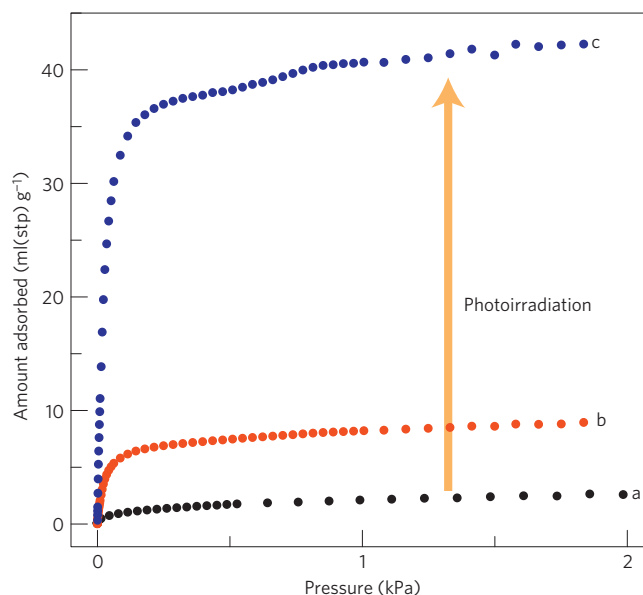
Figure 5 | *In situ* photoactivation of CID-N$_3$ with adsorption of oxygen.
Adsorption isotherms for O$_2$ at 77 K on dried CID-N$_3$ without (isotherm a)
and under (isotherm b) photoirradiation, and completely activated CID-N$_3$
(isotherm c). The photochemical conversion (15%) after the adsorption
measurement (isotherm b) was estimated by the ^{1}H-NMR spectrum of the
photoactivated sample. The isotherm for completely activated CID-N$_3$ (c)
was obtained from isotherms a and b considering the photochemical
conversion (15%).

strategy to produce PCPs with reactive open-shell atom sites such
as radicals and carbenes, which cannot be realized in conventional
synthetic conditions. Furthermore, regularly aligned electron-
deficient species in nanospace are of potential use in selective
adsorption for nucleophilic molecules and various topologically
controlled chemical reactions. These results will open up a new
dimension of porous compounds as platforms for various surface
conversions and selective guest trapping.

Methods

Measurements. ^{1}H and ^{13}C-NMR spectra were recorded on a spectrometer (JEOL
model JNM-ECS 400), operating at 399.8 and 100.5 MHz, respectively, using
tetramethylsilane as an internal reference. Infrared spectra were recorded on a
Fourier transform infrared spectrometer (JASCO model FT/IR-4200) using a
cryostat (Oxford cryostat MicrostatN) with neat samples or samples prepared in
KBr pellets. ESR spectra were recorded in vacuum at 77 K on an ESR spectrometer
(JEOL model JES-FA100). Thermogravimetric analyses were recorded (Rigaku
Thermo plus TG-8120) in the temperature range between 298 K and 673 K under a
nitrogen atmosphere at a heating rate of 5 K min^{-1}.

Synthesis of 5-azidoisophthalic acid (H$_2$N$_3$-ipa). H$_2$N$_3$-ipa was synthesized
according to a slightly modified published procedure[40]. A water solution (50 ml)
of sodium nitrite (2.0 g, 2.9 mmol) at 0 °C was dropwise added to a 2 M HCl
solution (500 ml) of 5-aminoisophthalic acid (5.0 g, 2.8 mmol), and the mixture
was stirred for 15 min at 0 °C. To the resulting yellow solution was slowly added
a water solution (50 ml) of sodium azide (1.9 g, 2.9 mmol) over 20 min, and the
mixture was stirred for 30 min at 0 °C and for 12 h at room temperature. The
resulting precipitates were collected by filtration and washed with water to give the
product (5.4 g, 94%). ^{1}H-NMR (400 MHz, DMSO-d_6): δ 7.73 (d, 2H, Ar), 8.19 (t,
1H, Ar), 13.50 (br, 2H, CO$_2$H); ^{13}C-NMR (100 MHz, DMSO-d_6): δ 123.99, 126.70,
133.56, 141.22, 166.34.

Synthesis of 5-nitrosoisophthalic acid (H$_2$NO-ipa). H$_2$NO-ipa was synthesized
according to the modified published procedure[41]. 5-aminoisophthalic acid
(181 mg, 1 mmol) was suspended in dichloromethane (5 ml). To this suspension,
oxone (1.23 g, 2 mmol) dissolved in water (10 ml) was added and the resulting
suspension was stirred for 20 min at room temperature. After separation of the
layers, the aqueous layer was extracted with dichloromethane three times. The
combined organic solution was washed with 1 N HCl and brine, dried over Na$_2$SO$_4$
and evaporated to dryness to give a crude product, which was subjected to recycling

preparative size-exclusion chromatography with tetrahydrofuran as an eluent.
The second fraction was collected and evaporated to leave H$_2$NO-ipa as solid
(23 mg, 12%). ^{1}H-NMR (400 MHz, DMSO-d_6): δ 8.56 (d, 2H, Ar), 8.86 (t, 1H,
Ar), 13.94 (br, 2H, CO$_2$H); ^{13}C-NMR (100 MHz, DMSO-d_6): δ 124.66, 133.67,
136.04, 164.88, 165.93.

Synthesis of {[Zn$_2$(N$_3$-ipa)$_2$(bpy)$_2$(DMF)$_{1.5}$]}$_n$ (CID-N$_3$). CID-N$_3$ was synthesized
according to a slightly modified published procedure[42]. On a DMF solution (2 ml)
of Zn(NO$_3$)$_2$·6H$_2$O (11.9 mg, 0.04 mmol) was carefully layered a MeOH solution
(2 ml) of H$_2$N$_3$-ipa (8.3 mg, 0.04 mmol) and bpy (6.2 mg, 0.04 mmol). Pale-yellow
block-shaped crystals were obtained in a few days. (Elemental analysis calculated
for C$_{40.5}$H$_{32.5}$N$_{11.5}$O$_{9.5}$Zn$_2$ (CID-N$_3$) C, 50.51; H, 3.40; N, 16.73; found C,
50.44; H, 3.43; N, 16.50.)

Gas adsorption measurement. The sorption isotherm measurements for N$_2$,
O$_2$, CO, CO$_2$ and C$_2$H$_2$ were made using an automatic volumetric adsorption
apparatus (BELSORP-18PLUS; Bel Japan) connected to a cryostat system. A known
weight (~100 mg) of the as-synthesized CID-N$_3$ was placed on a copper plate,
then the sample was dried under high vacuum (below 10^{-2} Pa) at 120 °C for 6 h
to remove the solvated DMF molecules. The sample on the copper plate was set
in a cryostat system and heated under high vacuum (below 10^{-3} Pa) at 80 °C for
2 h before the measurements, then the temperature was set at the measurement
temperature. The change of the pressure was monitored and the degree of
adsorption was determined by the decrease of the pressure at the equilibrium state.
In situ photoirradiation on the sample was conducted through a quartz window
on the cryostat system with an ultrahigh-pressure Hg lamp. The measurement
temperatures were controlled in the range from 400 to 50 K by a closed-He-cycle
refrigerator-based cryostat.

References

1. Schüth, F., Sing, K. S. W. & Weitkamp, J. *Handbook of Porous Solids*
   (Wiley-VCH, 2002).
2. Rowsell, J. L. C., Spencer, E. C., Eckert, J., Howard, J. A. K. & Yaghi, O. M.
   Gas adsorption sites in a large-pore metal–organic framework. *Science* **309,**
   1350–1354 (2005).
3. Serre, C. *et al.* Role of solvent–host interactions that lead to very large swelling
   of hybrid frameworks. *Science* **315,** 1828–1831 (2007).
4. Yang, Q., Kapoor, M. P. & Inagaki, S. Sulfonic acid-functionalized mesoporous
   benzene–silica with a molecular-scale periodicity in the walls. *J. Am. Chem. Soc.*
   124, 9694–9695 (2002).
5. Alauzun, J., Mehdi, A., Reyé, C. & Corriu, R. J. P. Mesoporous materials with an
   acidic framework and basic pores. A successful cohabitation. *J. Am. Chem. Soc.*
   128, 8718–8719 (2006).
6. Georgiev, P. A., Albinati, A., Mojet, B. L., Ollivier, J. & Eckert, J. Observation
   of exceptionally strong binding of molecular hydrogen in a porous material:
   Formation of an η^2-H$_2$ complex in a Cu-exchanged ZSM-5 zeolite.
   J. Am. Chem. Soc. **129,** 8086–8087 (2007).
7. Maji, T. K., Matsuda, R. & Kitagawa, S. A flexible interpenetrating
   coordination framework with a bimodal porous functionality. *Nature Mater.*
   6, 142–148 (2007).
8. Asefa, T., MacLachlan, M. J., Coombs, N. & Ozin, G. A. Periodic mesoporous
   organosilicas with organic groups inside the channel walls. *Nature* **402,**
   867–871 (1999).
9. Feng, X. *et al.* Functionalized monolayers on ordered mesoporous supports.
   Science **276,** 923–926 (1997).
10. Li, Q. *et al.* Docking in metal–organic frameworks. *Science* **325,** 855–859 (2009).
11. Matsuda, R. *et al.* Highly controlled acetylene accommodation in a
    metal–organic microporous material. *Nature* **436,** 238–241 (2005).
12. Xiang, S., Zhang, Y., Xin, Q. & Li, C. Asymmetric epoxidation of allyl alcohol
    on organic–inorganic hybrid chiral catalysts grafted onto the surface of silica
    and in the mesopores of MCM-41. *Angew. Chem. Int. Ed.* **41,** 821–824 (2002).
13. Che, S. *et al.* A novel anionic surfactant templating route for synthesizing
    mesoporous silica with unique structure. *Nature Mater.* **2,** 801–805 (2003).
14. Bradshaw, D., Claridge, J. B., Cussen, E. J., Prior, T. J. & Rosseinsky, M. J.
    Design, chirality, and flexibility in nanoporous molecule-based materials.
    Acc. Chem. Res. **38,** 273–282 (2005).
15. Kuschel, A., Sievers, H. & Polarz, S. Amino acid silica hybrid materials with
    mesoporous structure and enantiopure surfaces. *Angew. Chem. Int. Ed.* **47,**
    9513–9517 (2008).
16. Moss, R. A., Platz, M. S. & Jones, M. Jr *Reactive Intermediate Chemistry*
    (Wiley-Interscience, 2004).
17. Yaghi, O. M. *et al.* Reticular synthesis and the design of new materials. *Nature*
    423, 705–714 (2003).
18. Férey, G. Hybrid porous solids: Past, present, future. *Chem. Soc. Rev.* **37,**
    191–214 (2008).

19. Dalgarno, S. J., Power, N. P. & Atwood, J. L. Metallo-supramolecular capsules. *Coord. Chem. Rev.* **252,** 825–841 (2008).

20. Morris, R. E. & Wheatley, P. S. Gas storage in nanoporous materials. *Angew. Chem. Int. Ed.* **47,** 4966–4981 (2008).

21. Nouar, F. *et al.* Supermolecular building blocks (SBBs) for the design and synthesis of highly porous metal–organic frameworks. *J. Am. Chem. Soc.* **130,** 1833–1835 (2008).

22. Kitagawa, S., Kitaura, R. & Noro, S-i. Functional porous coordination polymers. *Angew. Chem. Int. Ed.* **43,** 2334–2375 (2004).

23. Yang, S. *et al.* Cation-induced kinetic trapping and enhanced hydrogen adsorption in a modulated anionic metal–organic framework. *Nature Chem.* **1,** 487–493 (2009).

24. Mulfort, K. L. & Hupp, J. T. Chemical reduction of metal–organic framework materials as a method to enhance gas uptake and binding. *J. Am. Chem. Soc.* **129,** 9604–9605 (2007).

25. Halder, G. J., Kepert, C. J., Moubaraki, B., Murray, K. S. & Cashion, J. D. Guest-dependent spin crossover in a nanoporous molecular framework material. *Science* **298,** 1762–1765 (2002).

26. Dincă, M. & Long, J. R. High-enthalpy hydrogen adsorption in cation-exchanged variants of the microporous metal–organic framework $Mn_3[(Mn_4Cl)_3(BTT)_8(CH_3OH)_{10}]_2$. *J. Am. Chem. Soc.* **129,** 11172–11176 (2007).

27. Lee, Y-G., Moon, H. R., Cheon, Y. E. & Suh, M. P. A comparison of the H_2 sorption capacities of isostructural metal–organic frameworks with and without accessible metal sites: $[\{Zn_2(abtc)(dmf)_2\}_3]$ and $[\{Cu_2(abtc)(dmf)_2\}_3]$ versus $[\{Cu_2(abtc)\}_3]$. *Angew. Chem. Int. Ed.* **47,** 7741–7745 (2008).

28. Bradshaw, D., Warren, J. E. & Rosseinsky, M. J. Reversible concerted ligand substitution at alternating metal sites in an extended solid. *Science* **315,** 977–980 (2007).

29. Seo, J. S. *et al.* A homochiral metal–organic porous material for enantioselective separation and catalysis. *Nature* **404,** 982–986 (2000).

30. Hasegawa, S. *et al.* Three-dimensional porous coordination polymer functionalized with amide groups based on tridentate ligand: Selective sorption and catalysis. *J. Am. Chem. Soc.* **129,** 2607–2614 (2007).

31. Ingleson, M. J. *et al.* Generation of a solid Brønsted acid site in a chiral framework. *Chem. Commun.* 1287–1289 (2008).

32. Kawamichi, T., Haneda, T., Kawano, M. & Fujita, M. X-ray observation of a transient hemiaminal trapped in a porous network. *Nature* **461,** 633–635 (2009).

33. Wang, Z. & Cohen, S. M. Postsynthetic modification of metal–organic frameworks. *Chem. Soc. Rev.* **38,** 1315–1329 (2009).

34. Seo, J., Matsuda, R., Sakamoto, H., Bonneau, C. & Kitagawa, S. A pillared-layer coordination polymer with a rotatable pillar acting as a molecular gate for guest molecules. *J. Am. Chem. Soc.* **131,** 12792–12800 (2009).

35. Gritsan, N. P. & Platz, M. S. Kinetics, spectroscopy, and computational chemistry of arylnitrenes. *Chem. Rev.* **106,** 3844–3867 (2006).

36. Sasaki, A., Mahé, L., Izuoka, A. & Sugawara, T. Chemical consequences of arylnitrenes in the crystalline environment. *Bull. Chem. Soc. Jpn* **71,** 1259–1275 (1998).

37. Harder, T., Wessig, P., Bendig, J. & Stösser, R. Photochemical reactions of nitroso oxides at low temperatures: The first experimental evidence for dioxaziridines. *J. Am. Chem. Soc.* **121,** 6580–6588 (1999).

38. Inui, H., Irisawa, M. & Oishi, S. Reaction of (4-nitrophenyl)nitrene with molecular oxygen in low-temperature matrices: First IR detection and photochemistry of aryl nitroso oxide. *Chem. Lett.* **34,** 478–479 (2005).

39. Dunkin, I. R. & Thomson, P. C. P. Pentafluorophenyl nitrene: A matrix isolated aryl nitrene that does not undergo ring expansion. *J. Chem. Soc. Chem. Commun.* 1192–1193 (1982).

40. Lamara, K. & Smalley, R. K. 3H-Azepines and related systems. Part 4. Preparation of 3H-azepin-2-ones and 6H-azepino[2,1-b]quinazolin-12-ones by photo-induced ring expansions of aryl azides. *Tetrahedron* **47,** 2277–2290 (1991).

41. Priewisch, B. & Rueck-Braun, K. Efficient preparation of nitrosoarenes for the synthesis of azobenzenes. *J. Org. Chem.* **70,** 2350–2352 (2005).

42. Horike, S., Tanaka, D., Nakagawa, K. & Kitagawa, S. Selective guest sorption in an interdigitated porous framework with hydrophobic pore surfaces. *Chem. Commun.* 3395–3397 (2007).

Author contributions

H.S., R.M. and S.K. conceived the project. H.S. and R.M. prepared and analysed all compounds described and carried out the sorption, spectroscopic measurements and photochemical experiments. K.S. and M.T. assisted the crystallographic study using synchrotron X-rays. H.S., R.M. and S.K. designed the study, analysed the data and wrote the paper.

Additional information

The authors declare no competing financial interests. Supplementary crystallographic data for this paper has been deposited at the Cambridge Crystallographic Data Centre under deposition numbers CCDC 778975 (CID-N3) and CCDC 778976 (photoactivated CID-N3). Supplementary information accompanies this paper on www.nature.com/naturematerials. Reprints and permissions information is available online at http://npg.nature.com/reprintsandpermissions. Correspondence and requests for materials should be addressed to R.M. and S.K.